



# Synthesis, structural characterization, encapsulation in zeolite Y and catalytic activity of an oxidovanadium(V) complex with a tribasic pentadentate ligand

Mannar R. Maurya<sup>a,\*</sup>, Manisha Bisht<sup>a</sup>, Nikita Chaudhary<sup>a</sup>, Fernando Avecilla<sup>b</sup>, Umesh Kumar<sup>c</sup>, Hua-Fen Hsu<sup>c</sup>

<sup>a</sup> Department of Chemistry, Indian Institute of Technology Roorkee, Roorkee 247 667, India

<sup>b</sup> Departamento de Química Fundamental, Universidad de Coruña, Campus de A Zapateira, 15071 A Coruña, Spain

<sup>c</sup> Department of Chemistry, National Cheng Kung University, #1 University Road, Tainan 701, Taiwan

## ARTICLE INFO

### Article history:

Received 14 August 2012

Accepted 9 February 2013

Available online 22 February 2013

### Keywords:

Oxidovanadium(V) complex

Crystal structure

Zeolit-Y encapsulated complex

Oxidation of styrene

Oxidation of methyl phenyl sulfide

Oxidation of diphenyl sulfide

## ABSTRACT

Reaction of  $[V^{IV}O(acac)_2]$  with  $H_3hap-dahp$  (**1**: Schiff base derived from 2-hydroxyacetophenone and 1,3-diamino-2-hydroxypropane) in methanol under aerobic conditions resulted in the formation of the complex  $[V^{VO}(hap-dahp)]$  (**1**). Treatment of **1** with vanadium(IV) exchanged zeolite Y followed by aerial oxidation gave the encapsulated oxidovanadium(V) complex  $[V^{VO}(hap-dahp)]-Y$  (**2**) in the nanocavity of zeolite Y. Elemental analysis, spectroscopic (IR, electronic,  $^1H$  and  $^{51}V$  NMR) studies, scanning electron micrographs and X-ray diffraction patterns have been used to characterize these complexes, which have a distorted octahedral structure, confirming the tribasic  $O_3N_2$  binding mode of the ligand. The encapsulated complex  $[V^{VO}(hap-dahp)]-Y$  (**2**) catalyzes the oxidation of styrene, methyl phenyl sulfide and diphenyl sulfide using  $H_2O_2$  as an oxidant in good yield (82%, 98% and 81%, respectively). Styrene, under optimized reaction conditions, gave five reaction products, namely styrene oxide, benzaldehyde, 1-phenylethane-1,2-diol, benzoic acid and phenylacetaldehyde, while the organic sulfides gave the corresponding sulfoxides as the major product. The neat complex  $[V^{VO}(hap-dahp)]$  (**1**) also exhibits good catalytic activity for these substrates. The encapsulated complex showed a good recycling ability.

© 2013 Elsevier Ltd. All rights reserved.

## 1. Introduction

The coordination chemistry of vanadium has been studied extensively [1–3] due to its occurrence in the active site of enzymes (e.g. vanadate-dependent haloperoxidases and vanadium-nitrogenases) that are involved in various catalytic actions [4–6]. Many vanadium complexes provide a suitable structural and/or functional model for these enzymes [7]. Amongst the tetradentate ligands, salen type ( $H_2salen = N,N'$ -bis(salicylidene)ethane-1,2-diamine) ligands find a key place in the literature as complexes of such ligands have great potential as catalysts for oxido transfer reactions and other processes [8–10]. Vanadium complexes of *salan* ( $H_2salan =$  ligand obtained by reducing  $H_2salen$ ) type ligands have also shown good catalytic reactions for oxygen transfers and E-H activations [11–13]. The flexible nature of salen-type ligands has also provided opportunities to encapsulate various transition-metal complexes in the nanocavity of zeolites and to develop catalytic processes for various reactions [14–25]. Metallosalen complexes encapsulated in zeolite X have been used as catalysts for the oxidation of cyclooctane [14]. Ratnasamy and

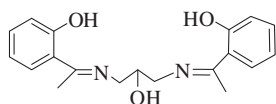
co-workers have used manganese(III) complexes of salen derivatives encapsulated in the cavity of zeolite X and zeolite Y for the oxidation of styrene under aerobic conditions using *tert*-butylhydroperoxide as an oxidant. They have also studied the effect of electron-withdrawing substituents, such as Cl, Br and  $NO_2$ , present on the aromatic ring on the rate of oxidation [15,16]. These complexes also catalyze the oxidation of phenol and *p*-xylene [26,27]. Zeolite Y encapsulated copper(II) [23], manganese(III) [25] and oxidovanadium(IV) [24] complexes of ligands derived from pyridoxal and various diamines have been reported from our laboratory for various oxidation reactions.

We have designed a ligand derived from 2-hydroxyacetophenone and 1,3-diamino-2-hydroxypropane ( $H_3hap-dahp$ , **1**; Scheme 1), similar to salen type ligands but with one more coordinating site whilst maintaining its flexible nature. The deprotonation behavior of the additional functional group and its participation or non-participation in coordination to metal ions controls the oxidation state of central metal ion [26].

We report herein the oxidovanadium(V) complex of **1**, its encapsulation in the super cages of zeolite Y and its characterization. The catalytic activities of neat as well as the encapsulated complex have been tested for the liquid phase oxidation of styrene, methyl phenyl sulfide and diphenyl sulfide. Styrene oxide, an oxidation product of styrene, is an important intermediate in organic

\* Corresponding author. Tel.: +91 1332 285327; fax: +91 1332 273560.

E-mail address: [rkmanfyc@iitr.ernet.in](mailto:rkmanfyc@iitr.ernet.in) (M.R. Maurya).

H<sub>3</sub>hap-dahp (I)

Scheme 1. Structure of ligand.

synthesis and in the manufacture of the perfumery chemical phenylethyl alcohol. Vanadium complexes are known to catalyze the oxidation of organic sulfides to sulfoxides and sulfones [13], a reaction also promoted by vanadium haloperoxidase enzymes.

## 2. Experimental

### 2.1. Materials and methods

V<sub>2</sub>O<sub>5</sub>, VOSO<sub>4</sub>·5H<sub>2</sub>O, (Loba Chemie, India), zeolite NaY (Si/Al = ~10) acetylacetone, 1,3-diamino-2-hydroxypropane (Aldrich, USA), 2-hydroxyacetophenone (Merck, Germany), methyl phenyl sulfide (Alfa Aesar, USA), styrene (Acros Organics, USA) and 30% aqueous H<sub>2</sub>O<sub>2</sub> (Qualigens, India) were used as obtained. All other chemicals and solvents used were of AR grade. [V<sup>IV</sup>O(acac)<sub>2</sub>] was prepared according to the method reported in the literature [27].

Elemental analyses (C, H and N) of the ligand and the complex were obtained by an Elementar model Vario-EL-III. IR spectra with a resolution of 2 cm<sup>-1</sup> were recorded as KBr pellets on a Nicolet 1100 FT-IR spectrometer after grinding the sample with KBr. A total of 32 scans were obtained to measure the spectra. Electronic spectra of the ligand and the neat complex were recorded in methanol. The electronic spectrum of the zeolite Y encapsulated complex was recorded in Nujol using a Shimadzu 1601 UV-Vis spectrophotometer by layering the mull of the sample inside of one of the cuvettes, whilst keeping the other one layered with Nujol as a reference. <sup>1</sup>H and <sup>13</sup>C NMR spectra were obtained on a Bruker 200 spectrometer, and <sup>51</sup>V NMR spectra on a Bruker Avance III 400 MHz spectrometer, with the common parameter settings. NMR spectra were usually recorded in DMSO-d<sub>6</sub>, and δ (<sup>51</sup>V) values are referenced relative to neat V<sup>V</sup>OCl<sub>3</sub> as an external standard. X-ray powder diffractograms of the zeolite containing samples were recorded using a Bruker AXS D8 advance X-ray powder diffractometer with a Cu Kα target. A scanning electron micrograph (SEM) of the catalyst was recorded on a Leo instrument, model 435VP. The sample was dusted on alumina and coated with a thin film of gold to prevent surface charging and to protect the surface material from thermal damage by the electron beam. A uniform thickness of about 0.1 mm was maintained. A constant voltage of 20 kV was applied so that only the outer surface of the zeolite Y was accessible. A Thermax Nicolet gas chromatograph with an HP-1 capillary column (30 m × 0.25 mm × 0.25 μm) was used to analyze the reaction products. The identity of the products was confirmed using a GC-MS model Perkin-Elmer, Clarus 500 by comparing the fragments of each product with the library available.

The percent conversion of the substrate and selectivity of the products were calculated from the GC data using the formulae presented elsewhere [25].

### 2.2. X-ray crystal structure determination

Three-dimensional X-ray data for [VO(hap-dahp)] (1) were collected on a Bruker SMART Apex CCD diffractometer at 100(2) K, using a graphite monochromator and Mo Kα radiation (λ = 0.71073 Å) by the φ-ω scan method. Reflections were measured from a hemisphere of data collected of frames each covering 0.3 degrees in ω. Of the 31174 reflections measured, all of which were corrected

**Table 1**  
Crystal data and structure refinement for [V<sup>V</sup>O(hap-dahp)] (1).

Formula	C <sub>19</sub> H <sub>19</sub> N <sub>2</sub> O <sub>4</sub> V
Formula weight	390.30
T, K	100(2)
Wavelength (Å)	0.71073
Crystal system	orthorhombic
Space group	Pbca
a (Å)	13.9677(3)
b (Å)	13.0077(3)
c (Å)	18.1778(4)
V (Å <sup>3</sup> )	3302.68(13)
Z	8
F(000)	1616
D <sub>calc</sub> (g cm <sup>-3</sup> )	1.570
μ (mm <sup>-1</sup> )	0.630
θ (°)	2.24–28.42
R <sub>int</sub>	0.0314
Crystal size (mm <sup>3</sup> )	0.36 × 0.26 × 0.18
Goodness-of-fit (GOF) on F <sup>2</sup>	1.050
R <sub>1</sub> <sup>a</sup>	0.0296
wR <sub>2</sub> (all data) <sup>b</sup>	0.0831
Largest differences peak and hole (e Å <sup>-3</sup> )	0.450 and -0.447

<sup>a</sup> R<sub>1</sub> = Σ|F<sub>o</sub> - F<sub>c</sub>|/Σ|F<sub>o</sub>|.

<sup>b</sup> wR<sub>2</sub> = {Σ[w(|F<sub>o</sub><sup>2</sup> - F<sub>c</sub><sup>2</sup>)|]/Σ[w(F<sub>o</sub><sup>4</sup>)]}<sup>1/2</sup>.

for Lorentz and polarization effects and for absorption by semi-empirical methods based on symmetry-equivalent and repeated reflections, 3619 independent reflections exceeded the significance level  $F/\sigma(F) > 4.0$ . Complex scattering factors were taken from the program package SHELXTL [28]. The structure was solved by direct methods and refined by full-matrix least-squares methods on F<sup>2</sup>. The non-hydrogen atoms were refined with anisotropic thermal parameters in all cases. The hydrogen atoms were left to refine freely. A final difference Fourier map showed no residual density outside: 0.450 and -0.447 e Å<sup>-3</sup>. Crystal data and details of the data collection and refinement for the new compound are collected in Table 1.

### 2.3. Preparations

#### 2.3.1. Preparation of H<sub>3</sub>hap-dahp (I)

A solution of 1,3-diamino-2-hydroxypropane (0.90 g, 10 mmol) dissolved in methanol (50 ml) was added to a solution of 2-hydroxyacetophenone (2.72 g, 20 mmol) dissolved in methanol (20 ml) and the reaction mixture was stirred at room temperature for 2 h. During this period a yellow solid slowly separated out. This was filtered off, washed thoroughly with water, followed by cold methanol and dried in a vacuum desiccator over silica gel. Yield 2.27 g (84%). Anal. Calc. for C<sub>19</sub>H<sub>22</sub>N<sub>2</sub>O<sub>3</sub> (326.40): C, 69.92; H, 6.79; N, 8.58. Found: C, 70.0; H, 6.8; N, 8.4%. <sup>1</sup>H NMR (DMSO-d<sub>6</sub>, δ/ppm): 13.56 (br, 2H, phenolic OH), 6.15–7.61 (m, 8H), 5.23 (br, 1H, -OH), 4.19 (m, 1H, -CH), 3.27 (m, 4H, -CH<sub>2</sub>), 2.13 (s, 6H, CH<sub>3</sub>).

#### 2.3.2. Preparation of [V<sup>V</sup>O(hap-dahp)] (1)

**2.3.2.1. Method A.** A filtered solution of VOSO<sub>4</sub>·5H<sub>2</sub>O (0.506 g, 2 mmol) in 10 ml methanol was added to a solution of H<sub>3</sub>hap-dahp (I) (0.652 g, 2 mmol) and triethylamine (0.606 g, 6 mmol) prepared in 10 ml of methanol, and the obtained reaction mixture was stirred for 2 h while bubbling air through it. The separated dark brown and off-white solid mixture was filtered off, washed with water, followed by cold methanol and dried in a vacuum desiccator over silica gel. Yield: 0.479 (59%). Anal. Calc. for C<sub>19</sub>H<sub>19</sub>N<sub>2</sub>O<sub>4</sub>V (390.31): C, 58.47; H, 4.91; N, 7.18. Found: C, 58.6; H, 4.9; N, 7.6%. For other details see Method B.

**2.3.2.2. Method B.** A stirred solution of H<sub>3</sub>hap-dahp (0.652 g, 2 mmol) in methanol (10 ml) was treated with [V<sup>IV</sup>O(acac)<sub>2</sub>] (0.530 g, 2 mmol) dissolved in methanol (10 ml), and the obtained reaction mixture was stirred while bubbling air through it. After 2 h of stirring, the separated dark brown solid was filtered, washed with cold methanol and dried. It was crystallized from methanol. Yield: 0.593 g (73%). *Anal.* Calc. for C<sub>19</sub>H<sub>19</sub>N<sub>2</sub>O<sub>4</sub>V (390.31): C, 58.47; H, 4.91; N, 7.18. Found: C, 58.2; H, 4.8; N, 7.4%. <sup>1</sup>H NMR (DMSO-d<sub>6</sub>, δ/ppm): 6.73–7.64 (m, 8H), 4.21 (m, 1H, –CH), 3.69 (m, 4H, –CH<sub>2</sub>), 2.35 (s, 6H, CH<sub>3</sub>). <sup>13</sup>C NMR (DMSO-d<sub>6</sub>, δ/ppm): 173.6 (C=N), 164.3, 132.8, 129.2, 119.43, 118.6, 117.0 (aromatic carbon), 53.3 (–CH), 39.3 (–CH<sub>2</sub>), 15.0 (–CH<sub>3</sub>).

### 2.3.3. Preparation of [V<sup>VO</sup>(hap-dahp)]-Y (2)

[V<sup>VO</sup>O]-Y [oxidovanadium(IV)-exchanged zeolite-Y] [24] (3.0 g) and H<sub>3</sub>hap-dahp (2.0 g) were mixed in methanol (100 ml) and the reaction mixture was heated under reflux for 14 h in an oil bath with stirring. After filtering, the resulting solid was Soxhlet extracted with methanol to remove any unreacted ligand. It was finally treated with hot DMF while stirring for 1 h, filtered and washed with DMF, followed by hot methanol. The uncomplexed metal ions present in the zeolite were removed by stirring with aqueous 0.1 M NaCl (150 ml) for 10 h. The resulting light brown solid was filtered, washed with hot methanol, followed by distilled water until no precipitate of AgCl was observed in the filtrate on treating with AgNO<sub>3</sub>. Finally it was dried at 120 °C for several hours. Recovered amount: 2.7 g. Found V (ICP-MS): 1.62%.

## 2.4. Catalytic activity studies

Zeolite Y encapsulated, [V<sup>VO</sup>(hap-dahp)]-Y (2) as well as the neat complex [V<sup>VO</sup>(hap-dahp)] (1) have been used as catalysts to carry out the oxidation of styrene, methyl phenyl sulfide and diphenyl sulfide. All reactions were carried out in a 50 ml two-necked glass reaction flask fitted with a water circulated condenser.

### 2.4.1. Oxidation of styrene

In a typical reaction, styrene (1.04 g, 10 mmol) and aqueous 30% H<sub>2</sub>O<sub>2</sub> (2.27 g, 20 mmol) were taken in 10 ml of acetonitrile and temperature of the reaction mixture was raised to 80 °C. After addition of catalyst (0.010 g) to the above reaction mixture, it was stirred and the obtained oxidized products were analyzed quantitatively by gas chromatography during the reaction by withdrawing small aliquots of the reaction mixture at one hour intervals. The identities of the products were confirmed by GC-MS and their quantifications were made on the basis of the relative peak area of the respective product.

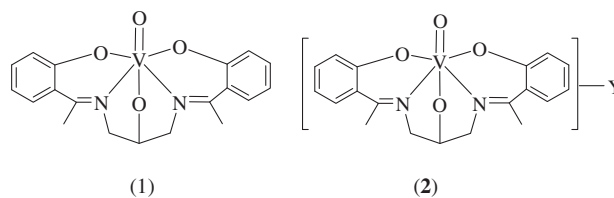
### 2.4.2. Oxidation of methyl phenyl sulfide and diphenyl sulfide

Methyl phenyl sulfide (1.24 g, 10 mmol) or diphenyl sulfide (1.86 g, 10 mmol), 30% aqueous H<sub>2</sub>O<sub>2</sub> (1.14 g, 10 mmol) and catalyst (0.0075 g) in acetonitrile were stirred at room temperature and the reaction was monitored by withdrawing samples at different time intervals and analyzing them quantitatively by gas chromatography. The identities of the products were confirmed as mentioned above.

## 3. Results and discussion

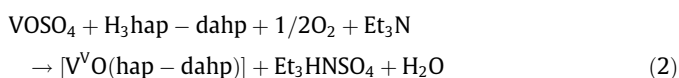
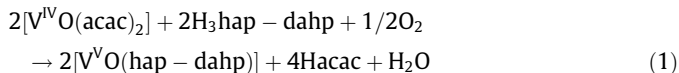
### 3.1. Synthesis and solid state characteristics

The reaction between equimolar amounts of [V<sup>IV</sup>O(acac)<sub>2</sub>] or VOSO<sub>4</sub> (in the presence of triethylamine) and H<sub>3</sub>hap-dahp (1) followed by aerial oxidation gives the brown oxidovanadium(V)



**Scheme 2.** Proposed structures for [V<sup>VO</sup>(hap-dahp)] (1) and the encapsulated complex [V<sup>VO</sup>(hap-dahp)]-Y (2).

complex [V<sup>VO</sup>(hap-dahp)] (1) (Scheme 2), where H<sub>3</sub>hap-dahp behaves as a tribasic pentadentate ligand; Eqs. (1) and (2):



The synthesis of the encapsulated complex in the nanocavity of zeolite Y involves: (i) exchange of [V<sup>IV</sup>O]<sup>2+</sup> with Na<sup>+</sup> of Na-Y in aqueous solution to form [V<sup>IV</sup>O]-Y and (ii) reaction of vanadium exchanged zeolite Y, i.e. [V<sup>IV</sup>O]-Y, with excess H<sub>3</sub>hap-dahp in methanol, where the ligand slowly enters into the super cages of zeolite Y due to its flexible nature and interacts with the vanadyl ion to give the vanadium(IV) complex, which on aerial oxidation gives [V<sup>VO</sup>(hap-dahp)]-Y (2) (Scheme 2). Extraction of the impure sample with methanol using a Soxhlet extractor removed any excess free ligand and the neat metal complex formed on the surface of the zeolite, if any. The remaining uncomplexed metal ions in zeolite were removed by exchanging with aqueous 0.1 M NaCl solution. As the impure sample was extracted well, the vanadium content (1.62%) found in 2 is only due to encapsulation of the vanadium complex in the cavities of zeolite-Y. Complex 1 is characterized on the basis of elemental analysis, spectroscopic (IR, UV-Vis, <sup>1</sup>H and <sup>51</sup>V NMR) data and single crystal X-ray diffraction analysis. Complex 2 is additionally characterized by FE-SEM, EDX and X-ray powder diffraction patterns.

### 3.2. Structure description of [V<sup>VO</sup>(hap-dahp)] (1)

Fig. 1 shows an ORTEP representation of [V<sup>VO</sup>(hap-dahp)] (1). The asymmetric unit contains one neutral vanadium complex. In the molecular structure, the vanadium center adopts a distorted six-coordinated octahedral geometry with the (hap-dahp) ligand coordinated through the two O<sub>phenoxy</sub>, two N<sub>imine</sub> and one O<sub>hydroxyl</sub> atoms. The ligand acts as a pentadentate phenol-containing ligand with (O,N,O,N,O)-donor atoms. Another (O,N,O,N,O)-donor ligand containing phenol groups presents a different coordination chemistry with the (V=O) ion [29], forming a dinuclear complex, perhaps due to the position of the imine group. The V=O bond [V(1)–O(3): 1.6023(10) Å] is characteristic of an oxo-type O atom with strong π bonding (see Table 2). The N=C bond lengths [N(1)–C(7): 1.2824(18) Å and N(2)–C(11): 1.2968(18) Å] are consistent with N=C double-bonds, the O–C bonds [O(1)–C(1): 1.3438(16) Å, O(2)–C(17): 1.3228(16) Å and O(4)–C(9): 1.4184(16) Å] with a single O–C character of these bonds, while the N–C bond lengths [N(1)–C(8): 1.4616(18) Å and N(2)–C(10): 1.4784(18) Å] are consistent with their single-bond character. The V–N<sub>imine</sub> bond, which is trans to the μ-oxo atom, is significantly longer [V(1)–N(1): 2.2734(11) Å] than the other N<sub>imine</sub> atom, which is trans to the O<sub>phenoxy</sub> atom [V(1)–N(2): 2.1220(12) Å] [12,26]. The tetragonal plane is best defined by O(1)–O(2)–N(2)–O(4) (mean deviation from the plane = 0.0371(5) Å), leaving the oxo atom, O(3), and the other

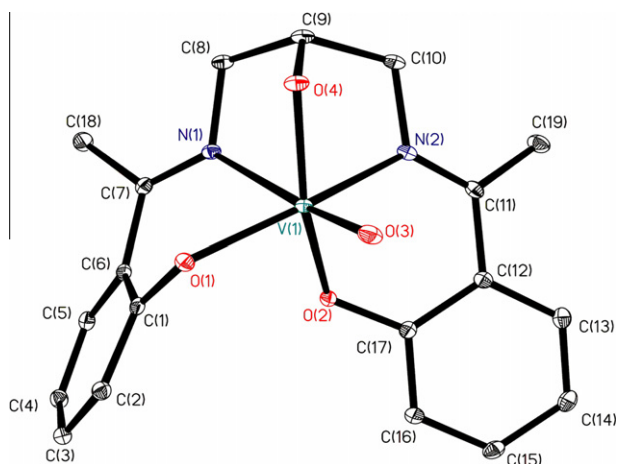


**Fig. 1.** ORTEP plot of the complex  $[V^{VO}(\text{hap-dahp})]$  (**1**). All non-hydrogen atoms are presented by their 30% probability ellipsoids. Hydrogen atoms are omitted for clarity.

**Table 2**

Bond lengths [Å] and angles [°] for  $[VO(\text{hap-dahp})]$  (**1**).

Bond lengths		Bond angles	
V(1)–O(3)	1.6023(10)	O(3)–V(1)–O(4)	95.74(5)
V(1)–O(4)	1.8627(10)	O(3)–V(1)–O(1)	99.41(5)
V(1)–O(1)	1.8776(11)	O(4)–V(1)–O(1)	109.19(4)
V(1)–O(2)	1.8931(9)	O(3)–V(1)–O(2)	100.65(5)
V(1)–N(2)	2.1220(12)	O(4)–V(1)–O(2)	153.92(5)
V(1)–N(1)	2.2734(11)	O(1)–V(1)–O(2)	88.06(4)
O(1)–C(1)	1.3438(16)	O(3)–V(1)–N(2)	100.33(5)
O(2)–C(17)	1.3228(16)	O(4)–V(1)–N(2)	77.11(4)
N(1)–C(7)	1.2824(18)	O(1)–V(1)–N(2)	158.53(4)
N(1)–C(8)	1.4616(18)	O(2)–V(1)–N(2)	80.08(4)
N(2)–C(11)	1.2968(18)	O(3)–V(1)–N(1)	169.67(5)
N(2)–C(10)	1.4784(18)	O(4)–V(1)–N(1)	75.35(4)
O(4)–C(9)	1.4184(16)	O(1)–V(1)–N(1)	79.07(4)
		O(2)–V(1)–N(1)	89.54(4)
		N(2)–V(1)–N(1)	82.97(4)

$N_{\text{imine}}$  atom, N(1), in the axial positions. The torsion angle of the plane containing C(5)–C(6)–C(7)–N(1) presents a sizeable deviation to 180°:  $-149.77(13)^\circ$ , while N(2)–C(11)–C(12)–C(13) is closer to 180°:  $-165.91(13)^\circ$ . The presence of methyl groups bonded to the carbon atoms of the imine bonding obstructs the formation of hydrogen bonds between the complexes in the crystal packing.

### 3.3. IR spectral studies

Complex **1** displays one sharp band at  $945\text{ cm}^{-1}$  due to the  $\nu(\text{V}=\text{O})$  mode. The zeolite Y framework displays major IR bands at 1140, 1040, 960, 785 and  $740\text{ cm}^{-1}$  [13,17,30] and because of these bands, the band due to  $\nu(\text{V}=\text{O})$  stretching in  $[V^{VO}(\text{hap-dahp})]$ -Y (**2**) could not be assigned unambiguously. However, other bands appearing in complex **2** are similar to **1**. The supporting information provides further details on the IR discussion.

### 3.4. Field-emission-scanning electron micrograph (FE-SEM) and energy dispersive X-ray analysis (EDX) studies

The field emission scanning electron micrograph of  $[V^{VO}(\text{hap-dahp})]$ -Y (**2**), along with the energy dispersive X-ray analysis (EDX) profile, is presented in Fig. 2. Accurate information on the morphological changes in terms of the exact orientation of the ligand coordinated to the metal ion has not been possible due to poor loading of the metal complex. However, it is clear from the micrograph that the vanadium complex entrapped zeolite has well defined crystals and there is no indication of the presence of any metal ions or complex on the surface. An energy dispersive X-ray analysis plot, evaluated semi-quantitatively, supports this conclusion as no vanadium or nitrogen contents were noted on the spotted surface in the plot for the catalyst. Only a small amount of carbon (ca. 6%) and no nitrogen on the spotted surface suggests the presence of a trace amount of solvent (methanol), with which it was finally washed after Soxhlet extraction. The amount of ca. 2% sodium suggests the exchange of the remaining free vanadium ion by the sodium ion during the re-exchange process (see Section 2).

### 3.5. Powder X-ray diffraction studies

The powder X-ray diffraction patterns of Na-Y,  $[V^{IV}O]$ -Y and encapsulated oxidovanadium(V) complex  $[V^{VO}(\text{hap-dahp})]$ -Y (**2**) were recorded at  $2\theta$  values between  $5^\circ$  and  $70^\circ$ , and the patterns are presented in Fig. 3. Essentially similar diffraction patterns of Na-Y,  $[V^{IV}O]$ -Y and encapsulated complex have been noticed, except for a slightly weaker intensity of the zeolite Y having the metal complex encapsulated. These observations indicate that the framework of the zeolite has not undergone any structural change during incorporation of the catalyst, hence the crystallinity of the zeolite Y is preserved during the encapsulation. No new peaks due to the encapsulated complex were detected in the zeolite Y

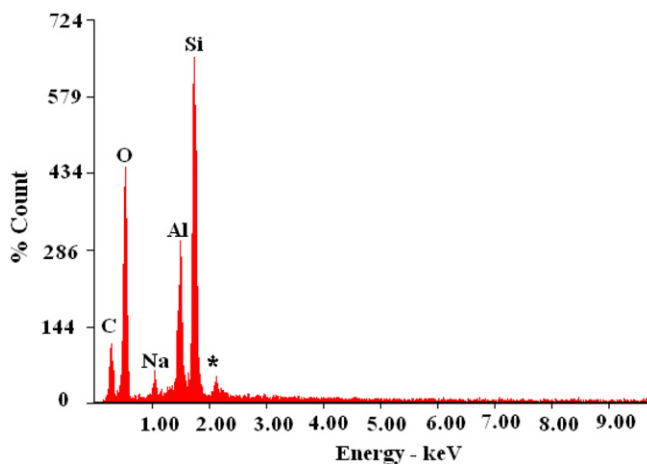
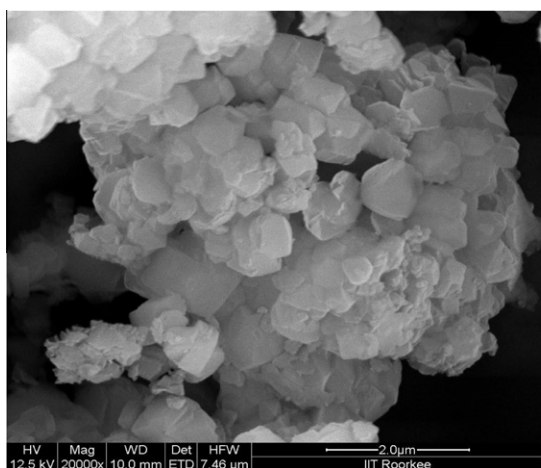


**Fig. 2.** Scanning electron micrograph (left) of  $[V^{VO}(\text{hap-dahp})]$ -Y (**2**) and energy dispersive X-ray analysis (EDX) (right). Asterisk in EDX shows the signal for gold.

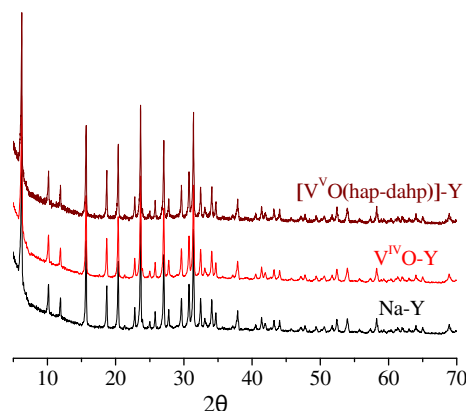


Fig. 3. XRD patterns of Na-Y,  $[V^{VO}(hap-dahp)]-Y$  and  $[V^{VO}(hap-dahp)]-Y$ .

encapsulated samples, possibly due to a very low percentage loading of the metal complex.

### 3.6. Electronic absorption spectral studies

Table 3 includes electronic spectral data of the ligand and the complexes, and Fig. 4 provides the spectrum of the encapsulated complex.  $H_3hap-dahp$  (**1**) exhibits four absorption bands in the UV region. The extinction coefficients of these bands suggest their interpretation as  $\pi \rightarrow \pi^*$  (260 and 280 nm) and  $n \rightarrow \pi^*$  (321 and 389 nm) transitions. The additional bands in the ligand are possibly due to splitting of these transitions. All these bands also appear in the spectrum of complex **1** with slight variations, while **2** exhibits only two bands at 222 and 279 nm, with a shoulder band at 370 nm. In addition, both complexes exhibit a ligand-to-metal charge transfer (LMCT) transition from the phenolate oxygen atom to an empty d-orbital of the vanadium atom at 485 nm (in **1**) and 480 nm (in **2**). As  $V^V$ -complexes have a  $3d^0$  configuration, no d  $\rightarrow$  d bands are not expected.

### 3.7. $^1H$ , $^{13}C$ and $^{51}V$ NMR Studies

The coordinating mode of  $H_3hap-dahp$  (**1**) was also confirmed by comparing its  $^1H$  NMR spectral patterns with those of the complex. The spectral data are presented in the experimental section.  $H_3hap-dahp$  shows two signals at 13.56 (s, 2H) and 5.35 ppm (broad, 1H) due to the phenolic and alcoholic OH, respectively. The absence of both signals in the complexes is in conformity with the coordination of the phenolic and alcoholic oxygen atoms to vanadium. Signals due to  $CH_3$ , CH,  $CH_2$  and aromatic protons of the ligand, as well as the complex, appear well within the expected regions.

The  $^{13}C$  NMR spectrum recorded for complex **1** contains 10 signals corresponding to the 19 carbon atoms of the molecules. The resonances at 15.0, 39.3, 53.3 and 173.6 ppm are due to the carbon atoms of  $CH_3$ ,  $CH_2$ , CH and  $C=N$ , respectively. Due to symmetry, only six signals are observed for the aromatic carbons in the expected regions, which is compatible with the proposed structure.

Table 3  
Electronic spectral data of the compounds.

Compound	Solvent	$\lambda_{max}$ (nm)/ $\epsilon$ (liter mol $^{-1}$ cm $^{-1}$ ) <sup>a</sup>
$H_3hap-dahp$ ( <b>1</b> )	MeOH	218( $3.98 \times 10^4$ ), 255( $1.55 \times 10^4$ ), 268( $1.37 \times 10^4$ ), 320( $5.09 \times 10^3$ ), 390( $6.6 \times 10^3$ )
$[V^{VO}(hap-dahp)]$ ( <b>1</b> )	MeOH	223( $8.2 \times 10^3$ ), 250(sh)( $5.77 \times 10^3$ ), 275( $3.22 \times 10^3$ ), 320( $1.6 \times 10^3$ ), 388( $1.08 \times 10^3$ ), 485( $0.93 \times 10^3$ )
$[V^{VO}(hap-dahp)]-Y$ ( <b>2</b> )	Nujol	222, 279, 370(sh), 480

<sup>a</sup> sh = Shoulder band.

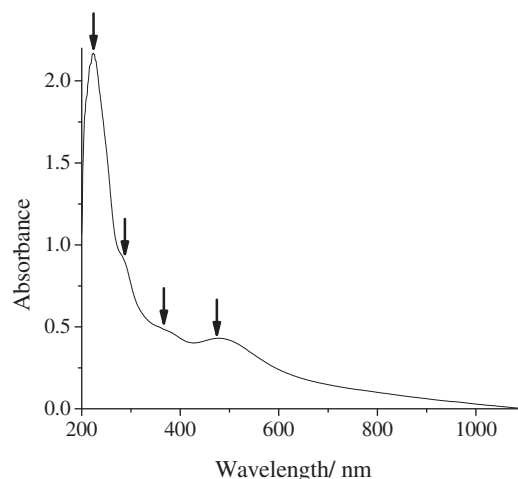


Fig. 4. Electronic spectrum of  $[V^{VO}(hap-dahp)]-Y$  (**2**) recorded after dispersal in Nujol.

We have also recorded the  $^{51}V$  NMR spectrum of  $[V^{VO}(hap-dahp)]$  (**1**) in  $DMSO-d_6$  using  $VOCl_3$  as an external standard. The  $^{51}V$  NMR spectrum of **1** dissolved in  $DMSO-d_6$  (ca. 4 mM) shows a strong resonance at  $\delta = -543$  ppm, characteristic of an O/N coordinated vanadium complex [31]. Owing to the quadrupole moment (spin 7/2) of the  $^{51}V$  nucleus, the resonance is slightly broadened; the line width at half-height is typically ca. 200 Hz, which may be considered comparatively narrow [31,32]. In order to see the effect of MeOH on the  $^{51}V$  NMR signal observed in  $DMSO-d_6$ , initially 0.25 eq (v/v) of MeOH was added, which resulted in two new signals at  $-503$  and  $-534$  ppm. Increasing the amount of MeOH to 0.5 and 0.75 eq (v/v) increased the intensity of these bands, slowly at the expense of the  $-543$  ppm resonance. Finally, this resonance completely disappeared upon addition of 1 eq (v/v) of MeOH and the resonances at  $-503$  (91.4%) and  $-534$  ppm (8.6%) became the main ones.

### 3.8. Reactivity of $[V^{VO}(hap-dahp)]$ towards $H_2O_2$

It is known that vanadium ( $[V^{VO}]^{2+}$ ,  $[V^{VO}]^{3+}$  or  $[V^{VO}_2]^+$ ) complexes react with  $H_2O_2$  to give the corresponding  $[V^{VO}(O_2)]^+$ -complexes, and it is normally assumed that the corresponding hydroperoxido-complex is the active catalyst which mediates oxygenation, including the oxidation of sulfides to sulfoxides and sulfones and the epoxidation of alkenes [33,34]. We have applied UV-Vis and  $^{51}V$  NMR spectroscopic studies and showed that addition of  $H_2O_2$  to a solution of  $[V^{VO}_2(hap-dahp)]$  in methanol/ $DMSO-d_6$  yields the oxidoperoxido species.

The changes in the absorption spectra during the dropwise addition of a 30%  $H_2O_2$  solution diluted in methanol to a methanolic solution of  $[V^{VO}(hap-dahp)]$  (**1**) are shown in Fig. 5. The charge transfer band appearing at ca. 485 nm slowly disappears with a decrease in intensity. Simultaneously, the weak shoulders appearing at 388 and 320 nm shift slightly to 392 and 325 nm, respectively, along with a slight increase in their intensities. These bands also

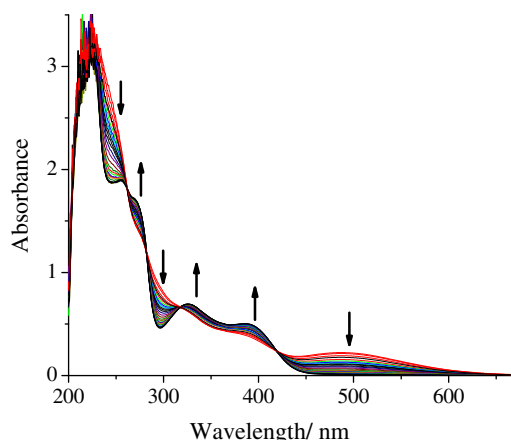


**Fig. 5.** Spectral changes observed during addition of aqueous 30%  $\text{H}_2\text{O}_2$  dissolved in 5 ml of methanol to 20 ml of ca.  $10^{-3}$  M solution of  $[\text{V}^{\text{VO}}(\text{hap-dahp})]$  in methanol.

result in the formation of two isosbestic points centered at 315 and 420 nm. With a marginal increase in the intensity, the band at 275 shifts to 268 nm while the extremely weak shoulder at ca. 250 nm sharpens with a decrease in intensity. Again these shifts generate two isosbestic points at 261 and 282 nm. These changes indicate the interaction of  $[\text{V}^{\text{VO}}(\text{hap-dahp})]$  (**1**) with  $\text{H}_2\text{O}_2$  and the plausible formation of  $[\text{V}^{\text{VO}}(\text{O}_2)(\text{hap-dahp})]^{2-}$  /  $[\text{V}^{\text{VO}}(\text{O}_2)(\text{Hhap-dahp})]^-$  in MeOH. However, among these possible peroxide species, the formation of  $[\text{V}^{\text{VO}}(\text{O}_2)(\text{Hhap-dahp})]^-$ , where the alcoholic oxygen of the amine residue remains protonated without coordinating to vanadium, is more likely as an oxidovanadium(IV) complex without a coordinating alcoholic oxygen is known [26].

The addition of 1 equiv of 30% aqueous  $\text{H}_2\text{O}_2$  to  $[\text{V}^{\text{VO}}(\text{hap-dahp})]$  dissolved in  $\text{DMSO-d}_6$  (ca. 4 mM) results in the broadening of the resonance at  $-543$  ppm. Upon further addition of 1 equiv of  $\text{H}_2\text{O}_2$ , a new resonance at  $-594$  ppm becomes visible along with the original peak. The original peak completely disappears after the addition of 3 equiv of  $\text{H}_2\text{O}_2$  and additions of 4 and 5 equiv of 30%  $\text{H}_2\text{O}_2$  make no difference in the spectra (Fig. 6). We tentatively

assign the resonance at  $-594$  ppm as being due to  $[\text{V}^{\text{VO}}(\text{O}_2)(\text{Hhap-dahp})]^-$  [35]. The formation of such a seven coordinated peroxido-vanadium(V) species upon addition of aqueous 30%  $\text{H}_2\text{O}_2$  to a methanolic solution of an oxidovanadium(IV) complex of a tetradentate ligand has been established by  $^{51}\text{V}$  NMR as well as in a theoretical study [12]. The solution acquires the original spectrum on either addition of 1 eq. of methyl phenyl sulfide or standing at room temperature for ca. 24 h, suggesting the reversibility of the system.

### 3.9. Catalytic activity studies

#### 3.9.1. Oxidation of styrene

The catalytic potential of the complex  $[\text{V}^{\text{VO}}(\text{hap-dahp})]\text{-Y}$  (**2**) was tested for the oxidation of styrene. Its catalytic oxidation in the presence of  $\text{H}_2\text{O}_2$  gave styrene oxide, benzaldehyde, 1-phenylethane-1,2-diol, benzoic acid and phenylacetaldehyde; Scheme 3. These products of styrene oxidation were previously observed by us and others as well [24,36–39].

In order to achieve suitable reaction conditions for a maximum oxidation of styrene, four different parameters, viz. amount of oxidant (mol of  $\text{H}_2\text{O}_2$  per mol of catalyst), catalyst, solvent and temperature of the reaction were tested. Table 4 (and Figs. S1 to S3 of the supporting information) summarizes the various conditions and conversions obtained.

Thus, for the maximum oxidation of 10 mmol of styrene, the following conditions were considered an adequate: catalyst (0.010 g),  $\text{H}_2\text{O}_2$  (2.27 g, 20 mmol),  $\text{CH}_3\text{CN}$  (15 mL) and  $80^\circ\text{C}$  reaction temperature (i.e. entry No. 7 of Table 4). Under the optimized reaction conditions, the selectivity of the different oxidation products formed varies in the order: benzaldehyde (49%) > 1-phenylethane-1,2-diol (25%) > benzoic acid (15%) > styrene oxide (6%) > phenylacetaldehyde (5%); Table 5. The formation of benzaldehyde with the highest yield may be due to the nucleophilic attack of  $\text{H}_2\text{O}_2$  on the styrene oxide formed in the first step, followed by the cleavage of the intermediate hydroperoxy styrene. Benzaldehyde formation may also be facilitated by direct oxidative cleavage of the styrene side chain double bond via a radical mechanism. The formation of 1-phenylethane-1,2-diol is possible

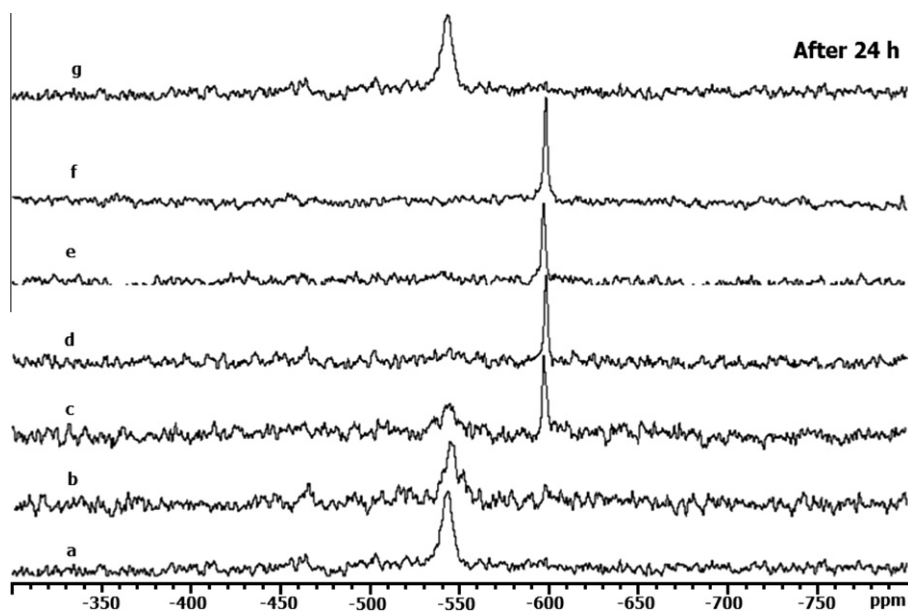
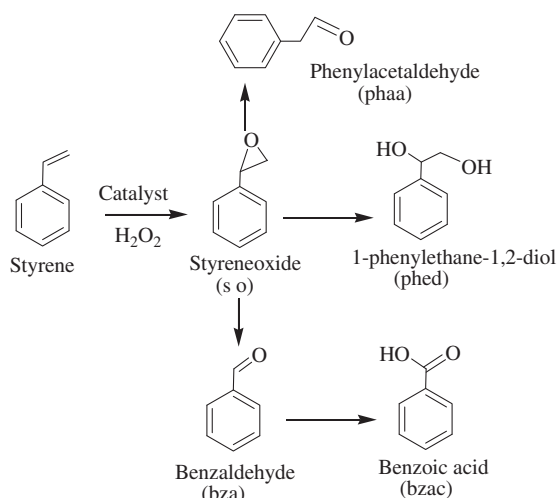


**Fig. 6.** Spectral changes observed during addition of 30%  $\text{H}_2\text{O}_2$ . (a) Spectrum of  $[\text{V}^{\text{VO}}(\text{hap-dahp})]$  (**1**) dissolved in  $\text{DMSO-d}_6$  (ca. 4 mM), (b) after addition 1 eq. of 30%  $\text{H}_2\text{O}_2$ , (c) after addition of 2 eq. of 30%  $\text{H}_2\text{O}_2$ , (d) after addition of 3 eq. of 30%  $\text{H}_2\text{O}_2$ , (e) after addition of 4 eq. of 30%  $\text{H}_2\text{O}_2$ , (f) after addition of 5 eq. of 30%  $\text{H}_2\text{O}_2$  and (g) after adding 1 eq. methyl phenyl sulfide to a solution of (f) or keeping the solution of (f) for 24 h.



**Scheme 3.** Oxidation products of styrene with  $\text{H}_2\text{O}_2$  catalyzed by  $[\text{V}^{\text{O}}(\text{hap-dahp})]\text{-Y}(2)$ .

**Table 4**

Conversion of 10 mmol (1.04 g) of styrene using  $[\text{V}^{\text{O}}(\text{hap-dahp})]\text{-Y}(2)$  as catalyst in a reaction time of 8 h under different reaction conditions.

Entry No.	Catalyst (g)	Temp. ( $^{\circ}\text{C}$ )	$\text{H}_2\text{O}_2$ (g, mmol)	$\text{CH}_3\text{CN}$ (ml)	Conv. (%)
1	0.010	80	1.14, 10	10	53.2
2	0.010	80	2.27, 20	10	71.5
3	0.010	80	3.41, 30	10	75.9
4	0.005	80	2.27, 20	10	34.3
5	0.015	80	2.27, 20	10	75.3
6	0.010	80	2.27, 20	5	52.7
7	0.010	80	2.27, 20	15	82.0
8	0.010	60	2.27, 20	15	48.3
9	0.010	70	2.27, 20	15	69.0

through hydrolysis of styrene oxide with water present in  $\text{H}_2\text{O}_2$  [13].

The conversion of styrene and the selectivity of the different reaction products using  $[\text{V}^{\text{O}}(\text{hap-dahp})]\text{-Y}$  as a catalyst under the optimized reaction conditions have been analyzed as a function of time and the results are presented in Fig. 7. It is clear from the plot that a selectivity of 80% of benzaldehyde has been obtained at a conversion of 15% of styrene in 1 h of reaction time. This selectivity slowly decreases with time and reaches 50% with an increase of the conversion of styrene to 82.0% in 8 h. The selectivity of styrene oxide (5%) and benzoic acid (3%) are relatively low and remains nearly constant over the conversion of styrene with time, while the formation of the other two products (i.e. 1-phenylethane-1,2-diol and phenyl acetaldehyde) are initially low, but slowly improve and reach 25% and 15%, respectively after 8 h of reaction time.

**Table 5**

Effect of catalysts on the oxidation of styrene, TOF and the product selectivity.

Catalyst	Substrate: oxidant ratio	Conv. (%)	TOF ( $\text{h}^{-1}$ )	Selectivity (%) <sup>a</sup>				
				bza	so	phea	bzac	phed
$[\text{V}^{\text{O}}(\text{hap-dahp})]$ (neat)	1:2	78	308	50	2	15	7	26
$[\text{V}^{\text{O}}(\text{hap-dahp})]\text{-Y}$	1:2	82	323	49	6	15	5	25
$[\text{V}^{\text{O}}(\text{hap-dahp})]\text{-Y}^{\text{b}}$	1:2	79	–	55	5	14	4	22
$[\text{V}^{\text{O}}(\text{hap-dahp})]\text{-Y}^{\text{c}}$	1:2	77	–	59	5	12	5	19
Without catalyst	1:2	4	–	82	4	7	3	4

<sup>a</sup> For abbreviations see Scheme 3.

<sup>b</sup> First cycle of used catalyst.

<sup>c</sup> Second cycle of used catalyst.

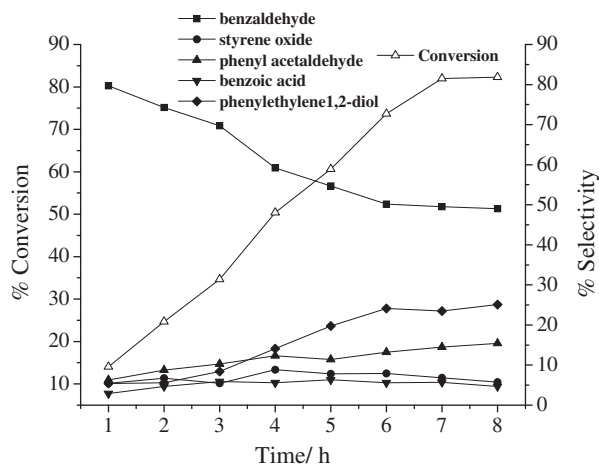


**Fig. 7.** Conversion of styrene and variation in the selectivity of different reaction products as a function of time using  $[\text{V}^{\text{O}}(\text{hap-dahp})]\text{-Y}$  as the catalyst.

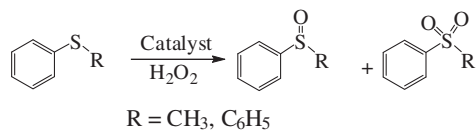
The encapsulated catalyst, separated from the reaction mixture after catalytic action, was washed with acetonitrile, dried and subjected to further catalytic reaction for the oxidation of styrene under similar conditions. The obtained results are presented in Table 5. It is clear from the table that the catalyst partially loses its catalytic activity during the recycling process. Nevertheless, the selectivity order is nearly maintained.

The neat complex  $[\text{V}^{\text{O}}(\text{hap-dahp})]$  (1), taking the same mole concentration as that used for the encapsulated complex, also exhibits a very comparable conversion of 78%, with a very similar selectivity of the different products (Table 5) as obtained by the encapsulated complex. A blank reaction under the above reaction conditions gave around 4% conversion. Thus, the neat complex as well as the encapsulated complex show good performance, but the possibility of the formation of oligomeric inactive species [40] and easier hydrolysis of the neat complex in the presence of aqueous  $\text{H}_2\text{O}_2$  relative to the encapsulated counterpart, and the recyclable nature as well as higher stability along with higher TOF value of the encapsulated complex make it significantly better over the neat complex.

### 3.9.2. Oxidation of methyl phenyl sulfide and diphenyl sulfide

The sulfur atom of the organic sulfide is electron rich and undergoes electrophilic oxidation catalyzed by several vanadium-dependent haloperoxidases [6,41,42] and model vanadium complexes [24]. Such oxidations of methyl phenyl sulfide and diphenyl sulfide were tested using  $[\text{V}^{\text{O}}(\text{hap-dahp})]\text{-Y}(2)$  as the catalyst and the corresponding sulfoxide as well as the sulfone were obtained, as shown in Scheme 4.

Again, the reactions were carried out under various conditions using 10 mmol (1.24 g) of methyl phenyl sulfide while varying the amount of catalyst (0.005, 0.0075 and 0.010 g), aqueous 30%



**Scheme 4.** Oxidation of methyl phenyl sulfide and diphenyl sulfide with H<sub>2</sub>O<sub>2</sub> catalyzed by [V<sup>VO</sup>(hap-dahp)]-Y (2).

**Table 6**

Conversion of methyl phenyl sulfide (1.24 g, 10 mmol) using [VO(hap-dahp)]-Y (2) as the catalyst in 3 h of reaction time under different reaction conditions.

Entry No.	Catalyst (g)	H <sub>2</sub> O <sub>2</sub> (g, mmol)	CH <sub>3</sub> CN (ml)	Conversion (%)
1	0.0075	1.14, 10	10	68
2	0.0075	1.71, 15	10	73
3	0.0075	2.27, 20	10	82
4	0.0075	2.84, 25	10	83
5	0.005	2.27, 20	10	70
6	0.010	2.27, 20	10	98
7	0.010	2.27, 20	05	82
8	0.010	2.27, 20	15	98

H<sub>2</sub>O<sub>2</sub> (10, 15, 20 and 25 mmol) and solvent (acetonitrile) volume (5, 10 and 15 ml), and the reaction was carried out at room temperature to obtain the maximum oxidation of the substrate. Table 6 (and Figs. S4 and S5 of the Supporting information) summarizes all the conditions and the conversion obtained under a particular set of conditions.

Entry 6 of Table 6 presents the optimized reaction conditions for 10 mmol of methyl phenyl sulfide, which are: substrate (1.24 g, 10 mmol), H<sub>2</sub>O<sub>2</sub> (2.27 g, 20 mmol), [V<sup>VO</sup>(hap-dahp)]-Y (0.010 g) and CH<sub>3</sub>CN (10 ml). The percent conversion of methyl phenyl sulfide under the optimized reaction conditions and the selectivity of the reaction products as a function of time are shown in Fig. 8. It is clear from the plot that both the products start to form with the conversion of methyl phenyl sulfide. However, the initial selectivity of 78% for methyl phenyl sulfoxide at 71% conversion of methyl phenyl sulfide in first half an hour moves towards the lower side for the initial 2 h and then partly improves and reaches 77% after 3 h of reaction time. Thus, the initially formed sulfoxide further reacts with H<sub>2</sub>O<sub>2</sub> present in the reaction mixture to give sulfone, but this reaction slowly suppresses after ca. 2 h and the selectivity for the formation of sulfoxide further improves. The

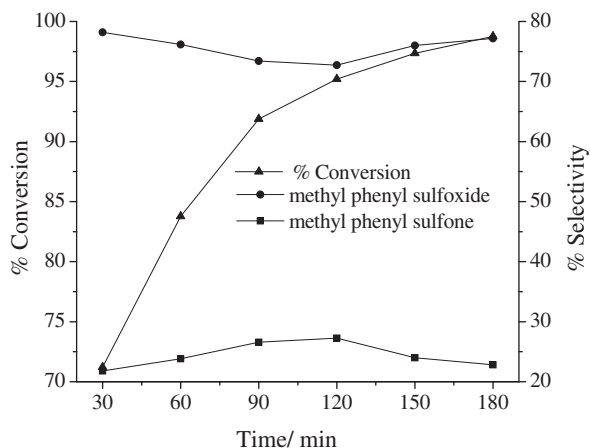


**Fig. 8.** Plots showing the percentage conversion of methyl phenyl sulfide, and the selectivity of the formation of methyl phenyl sulfoxide and methyl phenyl sulfone as a function of time. Reaction conditions: methyl phenyl sulfide (1.24 g, 10 mmol), H<sub>2</sub>O<sub>2</sub> (2.27 g, 20 mmol), [V<sup>VO</sup>(hap-dahp)]-Y (0.010 g) and acetonitrile (10 ml).

**Table 7**

Oxidation of methyl phenyl sulfide, conversion, TOF and product selectivity using the encapsulated and neat catalysts.

Catalyst (g)	TOF (h <sup>-1</sup> )	Conversion (%)	Selectivity (%) <sup>a</sup>	
			mpso	mpsn
[V <sup>VO</sup> (hap-dahp)]-Y	1036	98	77	23
[V <sup>VO</sup> (hap-dahp)]-Y <sup>b</sup>	–	97	74	26
[V <sup>VO</sup> (hap-dahp)]-Y <sup>c</sup>	–	96	75	25
[V <sup>VO</sup> (hap-dahp)]	1000	95	78	22
Blank	–	20	79	21

<sup>a</sup> Abbreviations: mpso = methyl phenyl sulfoxide, mpsn = methyl phenyl sulfone.

<sup>b</sup> First cycle of used catalyst.

<sup>c</sup> Second cycle of used catalyst.

**Table 8**

Conversion of diphenyl sulfide (1.86 g, 10 mmol) using [VO(hap-dahp)]-Y (2) as the catalyst in a reaction time of 7 h under different reaction conditions.

Entry No.	Catalyst (g)	H <sub>2</sub> O <sub>2</sub> (g, mmol)	CH <sub>3</sub> CN (ml)	Conversion (%)
1	0.005	1.14, 10	10	48.0
2	0.0075	1.14, 10	10	66
3	0.010	1.14, 10	10	55
4	0.0075	1.14, 10	15	81
5	0.0075	1.14, 10	20	71
6	0.0075	1.71, 15	15	59
7	0.0075	2.27, 20	15	39

overall selectivity of sulfone is only 23% and of sulfoxide it is 77% at a conversion of 98% at the end of 3 h.

The recycled encapsulated catalyst, after reactivating, was further used for the oxidation of methyl phenyl sulfide under similar conditions as mentioned above and the obtained results are presented in Table 7. It is clear from the table that the catalyst only partially loses its catalytic activity during recycling process. A blank reaction under similar conditions gave only 20% conversion. The neat complex [V<sup>VO</sup>(hap-dahp)] (1) also exhibits very good conversion (95%) of methyl phenyl sulfide, with a very similar selectivity of the different products as obtained by the encapsulated complex. However, the recyclable nature and higher turnover frequency (TOF) value of the encapsulated catalyst make it better over the neat complex.

Similarly for the oxidation of diphenyl sulfide, three different amounts of catalyst [V<sup>VO</sup>(hap-dahp)]-Y, oxidant and volume of solvent (acetonitrile) (see Table 8 and Figs. S6–S8) were considered

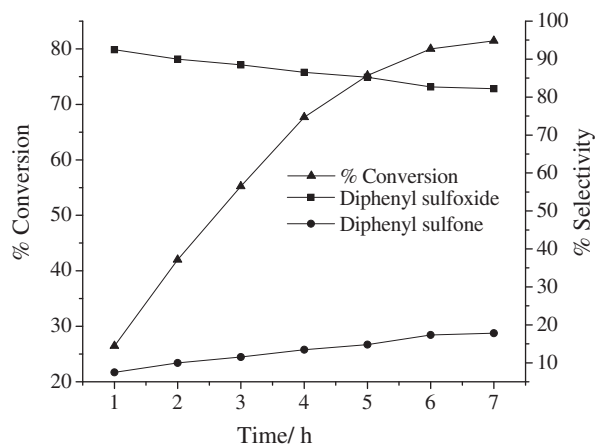


**Fig. 9.** Plot showing the percentage conversion of diphenyl sulfide and the selectivity of diphenyl sulfoxide and diphenyl sulfone formation as a function of time. Reaction conditions: diphenyl sulfide (1.86 g, 10 mmol), H<sub>2</sub>O<sub>2</sub> (1.14 g, 10 mmol), [V<sup>VO</sup>(hap-dahp)]-Y (0.0075 g) and 15 ml acetonitrile.

**Table 9**

Effect of different catalysts on the oxidation of diphenyl sulfide, conversion, TOF and product selectivity.

Catalyst (g)	TOF (h <sup>-1</sup> )	Conversion (%)	Selectivity (%) <sup>a</sup>	
			dpsO	dpsn
[V <sup>V</sup> O(hap-dahp)]-Y	488	81	82	18
[V <sup>V</sup> O(hap-dahp)]-Y <sup>b</sup>	–	77	80	20
[V <sup>V</sup> O(hap-dahp)]-Y <sup>c</sup>	–	75	79	21
[V <sup>V</sup> O(hap-dahp)]	450	75	85	15
Blank	–	5	90	10

<sup>a</sup> Abbreviations: dpsO = diphenyl sulfoxide, dpsn = diphenyl sulfone.<sup>b</sup> First cycle of used catalyst.<sup>c</sup> Second cycle of used catalyst.

and the reaction was carried out at room temperature. For 10 mmol (1.86 g.) of diphenyl sulfide, 0.075 g of catalyst and a H<sub>2</sub>O<sub>2</sub>:diphenyl sulfide molar ratio of 1:1 in 15 mL of acetonitrile, the reaction was found to give a maximum of 81% conversion of diphenyl sulfide in 7 h of reaction time at room temperature. The selectivity of sulfoxide and sulfone at this conversion is 82% and 18%, respectively.

Analysis of the conversion as a function of time, along with the selectivity of the reaction products (Fig. 9), shows that the initial selectivity of ca. 92% for the formation of diphenyl sulfoxide at ca. 25% conversion of diphenyl sulfide in the first hour of the reaction time slowly decreases with the elapse of time. After 7 h it reaches 82%, with a maximum conversion of 81% in 7 h. No further conversion or change in the selectivity of the products was noted after 7 h.

Again, the catalyst shows only partially loss in its catalytic activity after the recycling process (Table 9). A blank reaction under similar conditions gave only 5% conversion. The neat complex [V<sup>V</sup>O(hap-dahp)] (1) also exhibits a very good conversion (75%) of diphenyl sulfide with a very similar selectivity of the different products as obtained for the encapsulated complex.

#### 4. Conclusions

The oxidovanadium(V) complex [V<sup>V</sup>O(hap-dahp)] (1), where H<sub>3</sub>hap-dahp is the O<sub>3</sub>N<sub>2</sub> donor Schiff base obtained by the condensation of 2-hydroxyacetophenone and 1-3-diamino-2-hydroxypropane, has been synthesized and its molecular structure determined by single-crystal X-ray diffraction, confirming its distorted octahedral geometry. Complex 1 has been encapsulated in the super cages of zeolite Y and used as a catalyst for the oxidation of styrene, methyl phenyl sulfide and diphenyl sulfide with aqueous H<sub>2</sub>O<sub>2</sub> as an oxidant. A maximum of 82% conversion of styrene has been achieved under optimized reaction conditions, where the selectivity of the obtained five reaction products varies in the order: benzaldehyde (49%) > 1-phenylethane-1,2-diol (25%) > benzoic acid (15%) > styrene oxide (6%) > phenylacetaldehyde (5%). Under the optimized reaction conditions, a maximum of ca. 98% conversion of methyl phenyl sulfide, and ca. 81% of diphenyl sulfide has been achieved with significant amounts of the corresponding sulfoxide. The neat complex [V<sup>V</sup>O(hap-dahp)] is also a good catalyst for these substrates, along with a similar selectivity for the various products, but with significantly lower turnover frequencies. The encapsulated complex is recyclable at least up to two cycles of catalytic oxidation, but with a partial loss of activity.

#### Acknowledgements

M.R.M. is thankful to the Department of Science and Technology, Government of India, New Delhi for financial assistance (SR/

S1/IC-32/2010). MB acknowledges the Council of Scientific and Industrial Research (CSIR) for a NET–Junior Research fellowship.

#### Appendix A. Supplementary material

CCDC 888645 contains the supplementary crystallographic data for this paper. These data can be obtained free of charge via <http://www.ccdc.cam.ac.uk/conts/retrieving.html>, or from the Cambridge Crystallographic Data Centre, 12 Union Road, Cambridge CB2 1EZ, UK; fax: +44 1223 336 033; or e-mail: [deposit@ccdc.cam.ac.uk](mailto:deposit@ccdc.cam.ac.uk). Supplementary data associated with this article can be found in the online version, at <http://dx.doi.org/10.1016/j.poly.2013.02.036>.

#### References

- [1] D. Rehder, *Coord. Chem. Rev.* 182 (1999) 297.
- [2] M.R. Maurya, *Coord. Chem. Rev.* 237 (2003) 163.
- [3] D. Rehder, *J. Inorg. Biochem.* 80 (2000) 133.
- [4] R.R. Eady, in: H. Sigel, A. Sigel (Eds.), *Metal Ions in Biological Systems*, vol. 31, Marcel Dekker, New York, 1995.
- [5] A. Butler, in: J. Reedijk, E. Boiwan (Eds.), *Bioinorganic Catalysis*, second ed., Marcel Dekker, New York, 1999 (Chapter 5).
- [6] D. Rehder, *Bioinorganic Vanadium Chemistry*, John Wiley & Sons, New York, 2008, p. 115.
- [7] M.R. Maurya, A. Kumar, M. Ebel, D. Rehder, *Inorg. Chem.* 45 (2006) 5924 (and references therein).
- [8] L. Canali, D.C. Sherrington, *Chem. Soc. Rev.* 28 (1999) 85.
- [9] H. Gröger, *Chem. Rev.* 103 (2003) 2795.
- [10] P.G. Cozzi, *Chem. Soc. Rev.* 33 (2004) 410.
- [11] M.R. Maurya, J. Costa Pessoa, *J. Organomet. Chem.* 696 (2011) 244.
- [12] P. Adão, J. Costa Pessoa, R.T. Henriques, M.L. Kuznetsov, F. Avecilla, M.R. Maurya, U. Kumar, I. Correia, *Inorg. Chem.* 49 (2009) 3542.
- [13] M.R. Maurya, A. Kumar, J. Costa Pessoa, *Coord. Chem. Rev.* 255 (2011) 2315.
- [14] K.J. Balkus Jr., A.K. Khanrnamedova, K.M. Dixon, F. Bedioui, *Appl. Catal. A: Gen.* 143 (1996) 159.
- [15] S.P. Verkey, C. Ratnasamy, P. Ratnasamy, *J. Mol. Catal. A: Chem.* 135 (1998) 295.
- [16] C.R. Jacob, S.P. Varkey, P. Ratnasamy, *Microporous Mesoporous Mater.* 22 (1998) 465.
- [17] T. Joseph, D. Srinivas, C.S. Gopinath, S.B. Halligudi, *Catal. Lett.* 83 (2002) 209.
- [18] M.R. Maurya, M. Kumar, S.J.J. Titinchi, H.S. Abbo, S. Chand, *Catal. Lett.* 86 (2003) 97.
- [19] J. Poltowicz, K. Pamin, E. Tabor, J. Haber, A. Adamski, Z. Sojka, *Appl. Catal. A: Gen.* 299 (2006) 235.
- [20] H.M. Alvarez, L.F.B. Malta, M.H. Herbst, A. Horn Jr., O.A.C. Antunes, *Appl. Catal. A: Gen.* 326 (2007) 82.
- [21] M.R. Maurya, A.K. Chandrakar, S. Chand, *J. Mol. Catal. A: Chem.* 270 (2007) 225.
- [22] M. Salavati-Niasari, M.R. Ganjali, P. Norouzi, *J. Porous Mater.* 14 (2007) 423.
- [23] M.R. Maurya, B. Singh, P. Adão, F. Avecilla, J. Costa Pessoa, *Eur. J. Inorg. Chem.* (2007) 5720.
- [24] M.R. Maurya, P. Saini, A. Kumar, J. Costa Pessoa, *Eur. J. Inorg. Chem.* (2011) 4846.
- [25] M.R. Maurya, P. Saini, C. Haldar, F. Avecilla, *Polyhedron* 31 (2012) 710.
- [26] K.L. Smith, L.L. Borer, M.M. Olmstead, *Inorg. Chem.* 42 (2003) 7410.
- [27] R.A. Row, M.M. Jones, *Inorg. Synth.* 5 (1957) 113.
- [28] G.M. Sheldrick, *SHELXL-97: An Integrated System for Solving and Refining Crystal Structures from Diffraction Data (Revision 5.1)*, University of Göttingen, Germany, 1997.
- [29] S. Mukherjee, T. Weyhermüller, E. Bothe, P. Chaudhuri, *Eur. J. Inorg. Chem.* (2003) 1956.
- [30] A.P.A. Marques, E.R. Dockal, F.C. Skrobot, I.L.V. Rosa, *Inorg. Chem. Commun.* 10 (2007) 255.
- [31] D. Rehder, C. Weidemann, A. Duch, W. Priebsch, *Inorg. Chem.* 27 (1988) 584.
- [32] D. Rehder, in: P.S. Pregosin (Ed.), *Transition Metal Nuclear Magnetic Resonance*, Elsevier, New York, 1991.
- [33] A.G.J. Ligtenbarg, R. Hage, B.L. Feringa, *Coord. Chem. Rev.* 237 (2003) 89.
- [34] A. Butler, M.J. Clague, G.E. Meister, *Chem. Rev.* 94 (1994) 625.
- [35] M.R. Maurya, A.A. Khan, A. Azam, S. Ranjan, N. Mondal, A. Kumar, F. Avecilla, J. Costa Pessoa, *Dalton Trans.* 39 (2010) 1345.
- [36] R. Irie, Y. Ito, T. Katsuki, *Synlett* (1991) 265.
- [37] V. Hulea, E. Dumitriu, *Appl. Catal. A* 277 (2004) 99.
- [38] S.B. Kumar, S.P. Mirajkar, G.C.G. Pais, P. Kumar, R. Kumar, *J. Catal.* 156 (1995) 163.
- [39] M.R. Maurya, M. Bisht, A. Kumar, M.L. Kuznetsov, F. Avecilla, J. Costa Pessoa, *Dalton Trans.* 40 (2011) 6968.
- [40] L.F. Vilas Boas, J. Costa Pessoa, in: G. Wilkinson, R.D. Gillard, J.A. McCleverty (Eds.), *Comprehensive Coordination Chemistry*, Oxford, Pergamon, 1987, pp. 453–583.
- [41] M.A. Anderson, A. Willets, S. Allenmark, *J. Org. Chem.* 62 (1997) 8455.
- [42] H.B. ten Brink, H.E. Schoemaker, R. Wever, *Eur. J. Biochem.* 268 (2001) 132.